

A four-electrode liquid crystal device for 2π in-plane director rotation

C Desimpel¹, J Beeckman¹, H Desmet¹, K Neyts¹, R James² and F A Fernández²

¹ ELIS Department, Ghent University, St-Pietersnieuwstraat 41, B-9000 Gent, Belgium

² Department of Electronic and Electrical Engineering, University College London, Torrington Place, London WC1E 7JE, UK

E-mail: Chris.Desimpel@elis.UGent.be

Received 18 July 2005, in final form 31 August 2005

Published 24 October 2005

Online at stacks.iop.org/JPhysD/38/3976

Abstract

A novel type of liquid crystal device is described, based on a four-electrode unit, arranged in a hexagonal array. Full three-dimensional simulations were performed using a finite elements algorithm demonstrating a 2π rotation of the director in the plane parallel to the substrate surface. Applications for the device are situated in the field of multistable wave plates, spatial light modulators and electrically controllable anchoring.

(Some figures in this article are in colour only in the electronic version)

1. Introduction

A birefringent plate is a commonly used item in optical set-ups. Typical examples are a quarter-wave and a half-wave retardation plate. Liquid crystals have unique features which make them the ideal candidate for controllable wave plates. They are optically birefringent, and the orientation of the uniaxial axis can be controlled by an external electric field [1]. This allows the implementation of a reconfigurable wave plate without the need for mechanical moving parts.

The in-plane switching mode of liquid crystals [2] is based on the principle of a controllable wave plate. The director is originally oriented along the rubbing direction with a small pretilt and forms a uniform birefringent layer. The positive and negative electrodes are positioned on the bottom glass substrate forming a pattern of parallel interdigitated long stripes, at a small angle to the rubbing direction. Applying a voltage to the electrodes generates an electric field that rotates the director in the plane parallel to the surface. Although the in-plane switching mode has excellent characteristics for use in displays, its application as a controllable wave plate is limited. The rotation angle of the director is restricted to the angle between the rubbing direction and the direction perpendicular to the electrodes. The maximum rotation angle that can be reached in this way is $\pi/2$. Moreover, in the area above the electrodes a strong perpendicular field is present, and the director has a large tilt angle variation. This generates a two-dimensional director distribution and causes diffraction of

the incident light. Finally, removing the applied electric field causes the director to return to its original orientation.

Few devices have been demonstrated in which the rotation of the twist angle is not limited to $\pi/2$. Two examples are the cartwheel cell [3] and the tristable nematic liquid-crystal device [4]. This paper presents simulations of a new multistable device in which a 2π rotation of the director is possible.

2. Construction of a rotatable wave plate

The device consists of a layer of hexagonal electrode pads on the underside of a stack comprising a dielectric layer and a liquid crystal layer, sandwiched between two glass substrates (figure 1). The hexagonal electrodes are arranged in a hexagonal array in the xy -plane as illustrated in figure 2. The distance between two neighbouring hexagons, b , is $5\ \mu\text{m}$. The hexagons are of regular shape and have a side length, a , of $3\ \mu\text{m}$. The electrodes are grouped in four sets, marked with different grey levels in figure 2. An electric potential can be applied separately to each of the four groups.

The individual electrodes of each set are connected to a lower interconnection level through vias (metalized holes) in an insulating dielectric layer. It is assumed that the electric field due to the interconnection electrodes has a negligible influence on the director distribution. Therefore only the dashed rectangle in figure 1 has been simulated.

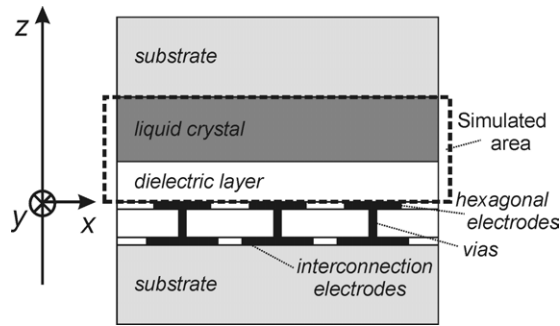


Figure 1. A schematic representation of the different layers in the described device with indication of the used coordinate axes and the hexagonal electrodes situated in the xy -plane.

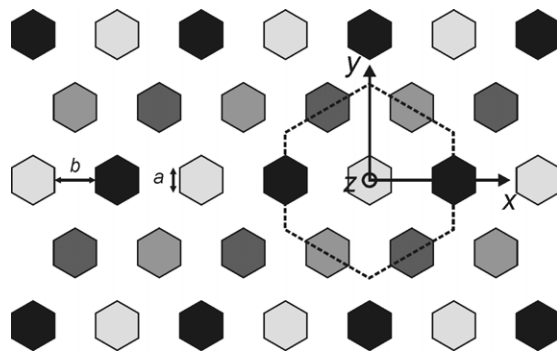


Figure 2. The hexagonal electrode pattern in the xy -plane. The four groups of electrodes are marked with different grey scales, with indication of a hexagonal building block.

The azimuthal angle between the positive x -axis and the projection of the liquid crystal director on the xy -plane is defined as the twist angle of the director. The angle between the director and its projection on the xy -plane is called the tilt angle. At the top and bottom surfaces of the liquid crystal layer an azimuthally degenerate planar anchoring surface is used. The aim of this alignment is to obtain a surface anchoring where the director has a tendency to lie in the horizontal plane (i.e. parallel to the xy -plane), but without a preferential azimuthal direction. This enables a 2π in-plane rotation of the director. Several techniques, as proposed in [5, 6], can be used to create such surfaces in order to avoid the effects of memory alignment [7].

3. Operating principle of the rotatable wave plate

The electrode topology described above, arranged in four sets of separately driven hexagonal pads, allows the implementation of a large variety of possible driving configurations. Here we restrict the study to the case in which the four sets are driven in pairs of two by two, so only three driving configurations are obtained. The three cases are shown in figure 3 and will be referred to as the driving configurations C_1 , C_2 and C_3 . The two grey levels in figure 3 indicate different potentials. The electrodes with the same potential form parallel lines, comparable with the parallel electrodes of the in-plane switching mode of liquid crystals. Changing the driving configuration rotates the electrode lines, and this in turn rotates the liquid crystal director.

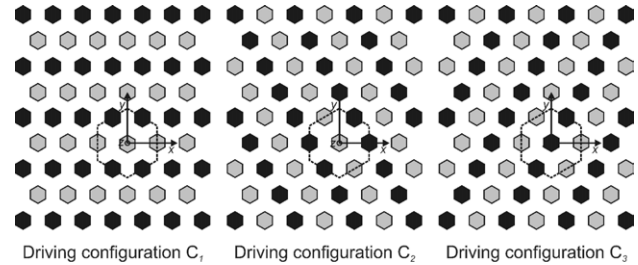


Figure 3. Three possibilities for driving the electrode sets in pairs two by two. The electrodes are situated in the xy -plane and the grey levels indicate different voltage levels.

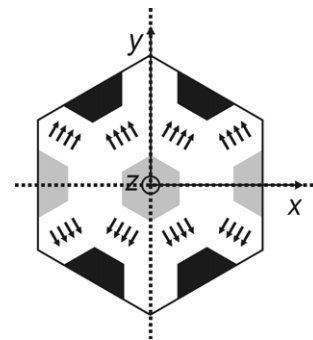


Figure 4. Indication of the approximate direction of the horizontal component of the electric field (represented by arrows) between neighbouring electrodes for driving configuration C_1 as well as the mirror planes xz and yz (represented by dotted lines).

The local electric field can be decomposed into two components: a horizontal field parallel to the xy -plane and a vertical field parallel to the z -axis. In between the parallel sides of two neighbouring electrodes with different potential levels, the horizontal electric field will be approximately in the direction perpendicular to the parallel sides as represented in figure 4. Taking into account that a liquid crystal makes no distinction between a positive or a negative electric field, it is clear from figure 4 that the average horizontal electric field is along the y -axis. The liquid crystal director will therefore align on average in this direction.

Figure 4 also reveals that in the case of driving configuration C_1 the xz -plane and the xy -plane are mirror planes. For driving configurations C_2 and C_3 , the average horizontal electric field makes an angle of $\pm\pi/3$ with the y -axis, and the mirror planes rotate from those shown in figure 4 by $\pm\pi/3$ about the z -axis.

Due to the hexagonal configuration, the angle between the average electric field in two driving configurations is always less than $\pi/2$. Consequently, a horizontal director rotation through an angle of 2π is indeed possible, as shown schematically in figure 5. For example, consider the situation that arises when C_2 is applied to a starting director configuration at t_0 , aligned in the y -direction. Applying C_2 causes the director to rotate towards the situation at t_1 , making an angle of $\pi/3$ with the positive y -axis. Now applying driving configuration C_3 will rotate the director towards t_2 , experiencing another rotation of $\pi/3$. Finally, applying C_1 aligns the director again along the y -axis, but its orientation has undergone a π rotation. Successive reapplication of C_2 , C_3

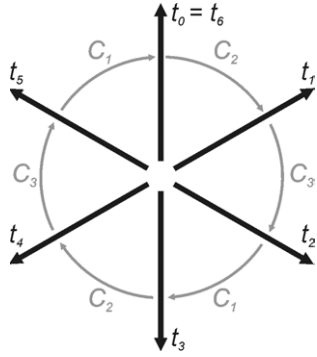


Figure 5. Illustration of the three directions along which the director can be aligned (opposite directions are physically equivalent) and the principle of a 2π director rotation by successive application of the three driving configurations.

and C_1 a second time results in the situation at t_6 . The director has returned to its original position after a 2π in-plane rotation.

4. Director simulations

Simulations have been performed using a dynamic three-dimensional liquid crystal director simulation tool, developed by the computer Modelling Group of University College London in the framework of the European project MonLCD (G5RD-CT-2000-00115). The method is based on an approach starting from the Oseen–Frank elastic distortion energy density [1] of the liquid crystal

$$f_d = \frac{1}{2} [k_{11}(\nabla \cdot \vec{n})^2 + k_{22}(\vec{n} \cdot \nabla \times \vec{n})^2 + k_{33}(\vec{n} \times \nabla \times \vec{n})^2], \quad (1)$$

which considers the three elastic constants k_{11} , k_{22} and k_{33} and a vectorial representation \vec{n} of the director distribution.

In the presence of an external electric field, there is an additional contribution to the total energy, the electric energy density of the liquid crystal [1], given by

$$f_e = \frac{1}{2} \epsilon_0 [\Delta \epsilon (\vec{n} \cdot \vec{E})^2 + \epsilon_{\perp} (\vec{E} \cdot \vec{E})], \quad (2)$$

where $\Delta \epsilon$ is the dielectric anisotropy and ϵ_{\perp} is the permittivity perpendicular to the director. Laplace's equation is solved over both the liquid crystal and the dielectric layers to yield the electric field \vec{E} .

Planar azimuthal degenerate anchoring of the director at the interface is modelled by a generalized form of the anchoring energy. A second order spherical harmonic approximation of the surface anchoring energy [8] leads to:

$$f_s = W_{\xi} (\vec{n} \cdot \vec{\xi})^2 + W_{\eta} (\vec{n} \cdot \vec{\eta})^2. \quad (3)$$

The so-called easy direction \vec{e} is oriented perpendicular to the orthogonal vectors $\vec{\xi}$ and $\vec{\eta}$. The vectors \vec{e} , $\vec{\xi}$ and $\vec{\eta}$ give the three principal axes of anchoring [8]. The anchoring strengths W_{ξ} and W_{η} give the cost for a deviation of the surface director away from the easy axis in the direction of $\vec{\xi}$ and $\vec{\eta}$. A choice of the parameters $W_{\xi} = 0$ and $\vec{\eta} = \vec{e}$ leads to a condition in which the surface director prefers to lie parallel to the surface but without any azimuthal constraint. For the second parameter we choose a value of $W_{\eta} = 5 \times 10^{-6} \text{ J m}^{-2}$, in the range of

values found in the literature [5–7]. This permits some tilting of the surface director, but this tilting has an associated energy penalty.

The total free energy of the liquid crystal layer can now be written down as in equation (4). It contains the contributions from the distortion and electric energy as well as the energy contribution of the surface anchoring:

$$F = \int_V [f_d - f_e] dV + \int_S f_s dS. \quad (4)$$

The dynamic evolution of the liquid crystal is governed by the dissipation equation:

$$\frac{\partial F}{\partial n_s} + \frac{\partial}{\partial n_s} \left(\frac{\gamma_1}{2} \int_V \dot{n}_{\mu} \dot{n}_{\mu} dV \right) = 0, \quad (5)$$

where γ_1 is the rotational viscosity of the liquid crystal. A finite elements approach is applied in order to solve the above system of differential equations for the director and electric fields. A detailed description of the algorithm used for the relaxation and the minimization of the total free energy and the calculation of the potential distribution in the liquid crystal and dielectric layer is given in [9–11].

Since the device is periodic only a single building block needs to be used for three-dimensional simulations. This minimum modelling window is a hexagon as represented on the right-hand side of figure 2. The side length of the hexagon is $11.77 \mu\text{m}$ and periodic boundary conditions are applied to the opposing faces. The calculations are executed on an irregular mesh of 23066 tetrahedral elements and 4675 nodes constructed with a commercial mesh generator.

The nematic liquid crystal used in the simulations is E7, with parameters $k_{11} = 12 \text{ pN}$, $k_{22} = 9 \text{ pN}$, $k_{33} = 19.5 \text{ pN}$, $\epsilon_{\parallel} = 19.6$, $\epsilon_{\perp} = 5.1$, $\gamma_1 = 150 \text{ mPa s}$, $n_o = 1.5231$ and $n_e = 1.75$ [12]. The thickness of the liquid crystal is chosen to be $2.1 \mu\text{m}$. For this thickness and for the wavelength of a HeNe-laser, the layer acts as a quarter-wave retardation plate when used in transmission and a half-wave retardation plate when used in reflection. The dielectric layer used had a thickness of $1.3 \mu\text{m}$ and a dielectric constant $\epsilon = 3.5$.

4.1. Simulated director distribution

Figure 6 illustrates the operation of the device, showing a π rotation of the director by applying successively the driving configurations C_1 , C_2 , C_3 and then again C_1 , each for 250 ms. Originally at $t = 0 \text{ ms}$, the director is oriented parallel to the y -axis. The voltage applied to an electrode is 0 V or 5 V depending on the desired driving configuration. The pictures show the orientation of the director as well as the potential distribution in the middle of the liquid crystal layer at the end of each time step in the sequence. The background colour indicates the potential distribution, the colour and length of the cones indicate the director tilt angle. The director distributions in step 1 at $t_0 = 250 \text{ ms}$ and step 4 at $t_3 = 1000 \text{ ms}$ both show an average director orientation parallel to the y -axis. However, in step 4 the director is rotated over an angle of π . At the intermediate steps $t_1 = 500 \text{ ms}$ and $t_2 = 750 \text{ ms}$, the average director orientation makes an angle of $\pi/6$ and $-\pi/6$, respectively, with the positive x -axis. Reapplying the

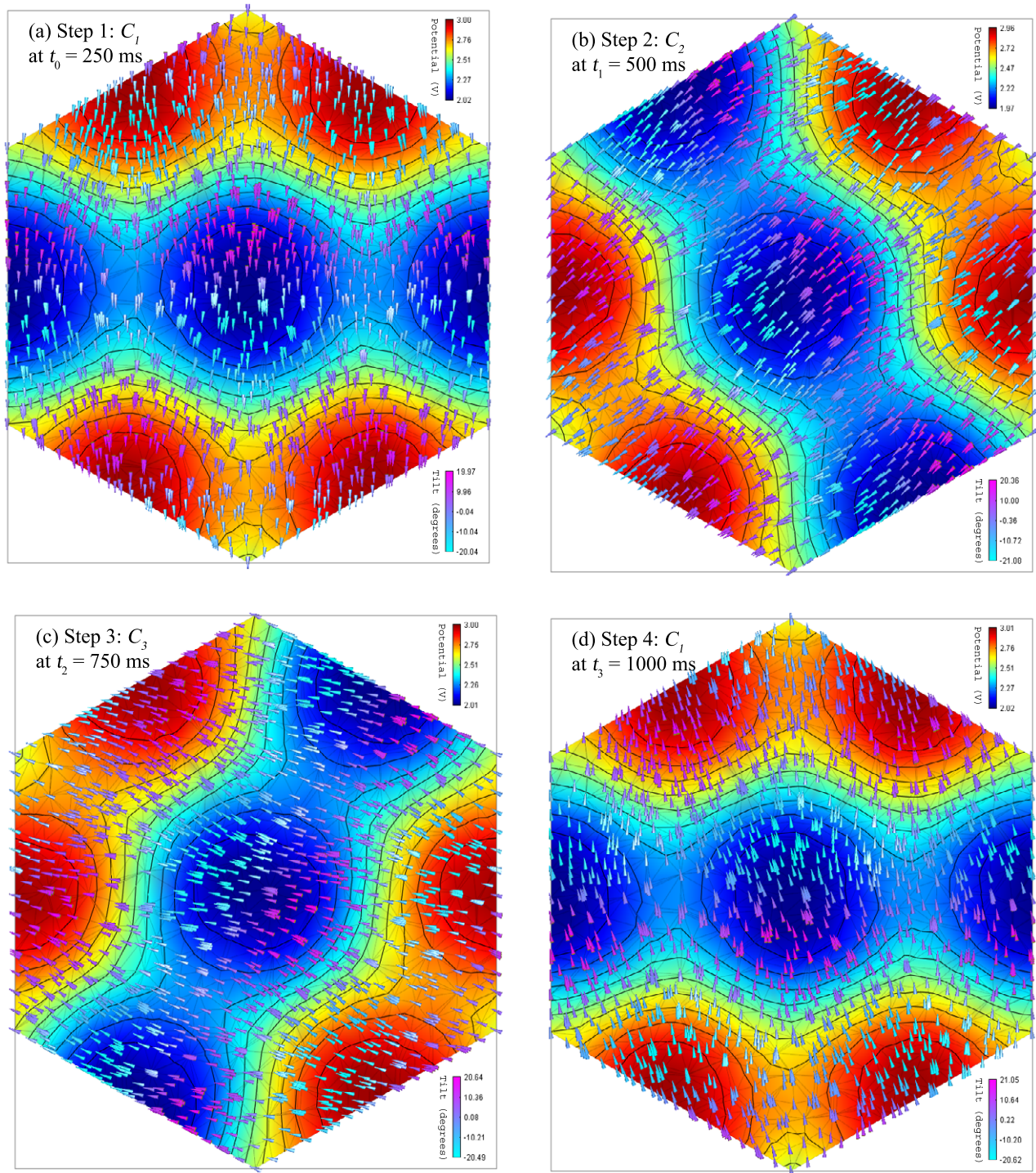


Figure 6. Director rotation over π by applying 4 consecutive driving configurations. The plots show the director and the potential distribution in a plane parallel to the xy -plane at $z = 2.35 \mu\text{m}$ (the middle of the liquid crystal layer) using the coordinate system as defined in figures 1 and 2. The background colour gives the potential variation (top right legend) with the equipotential lines. The small cones indicate the director distribution. The rotation of the cones is an indication of the local twist angle. The length and the colour of the rods (bottom right legend) indicate the tilt angle.

sequence of driving configurations C_2 , C_3 and C_1 results in a reorientation of the director to the original direction at t_6 after a 2π rotation of the director.

Switching from one driving configuration to another only requires a rotation over an angle of $\pi/3$. Physically there is no difference between steps 1 and 4. However, a limitation

of the maximum rotation angle below π would, in certain cases, require a longer and more time consuming rotation. For example, a rotation from step 3 via step 2 back to step 1 would require a rotation of $2\pi/3$.

As explained in section 3, the orientation of the mirror planes depends on the driving configuration. One type of

mirror plane (the xz -plane in figure 4) contains the centres of the hexagonal electrodes with the same potential. Due to symmetry, the electric field is parallel to the mirror plane and thus perpendicular to the average horizontal electric field of the driving configuration. To achieve a consistent director distribution, it is important that the director orientation is dominantly determined by elastic forces about this plane. Larger hexagons with reduced spacing lower the horizontal potential variation in the mirror plane. This decreases the horizontal electric field in the mirror plane and encourages the director to follow the average horizontal electric field orientation which is perpendicular to the mirror plane. A disadvantage of using larger electrode pads is that the region above the hexagonal pads where the horizontal potential variation is low is broadened, weakening the driving electric field at both sides of the mirror plane.

Figure 7 shows the potential and director distributions across several cut planes through the hexagonal unit to illustrate the potential distribution throughout the whole device in addition to the director distribution in the liquid crystal layer. In figures 7(a) and (b) the potential distribution is shown in the xy -plane at the bottom and in the middle of the dielectric layer. The slice plane in figure 7(a) is coincident with the electrode pads. Figures 7(c) and 7(d) show the director profile at the bottom and top of the liquid crystal layer. The middle of the liquid crystal layer is illustrated in figure 6(b).

It is important to note that the local horizontal electric field, given by the gradient of the potential distribution, makes an angle with the average horizontal electric field. At first sight, the local horizontal electric field between two electrodes on different potential levels appears to orient along the normal to the hexagonal electrode edges, with an angle of $\pm\pi/6$ with respect to the average electric field as schematically drawn in figure 4. On closer inspection of figures 7(a)–(d), however, it is found that the angle between the local horizontal electric field and the average orientation is less than $\pi/6$ and decreases with increasing z . At the bottom of the liquid crystal layer the twist of the local director is still spread across a range of almost $\pm\pi/6$ about the desired direction, while in the volume above the local director it is aligned almost homogeneously along the average direction of the horizontal electric field.

Near the electrodes, the vertical component of the electric field is strong. Figure 8(a) shows the director and the potential distribution in the absence of a dielectric layer. The plot shows that without the dielectric layer, the director above the electrodes tilts to an angle of almost $\pi/2$. When the applied voltage is removed, a tilt of $\pi/2$ can result in the formation of domains separated by defect lines, due to a relaxation of the director in opposite directions in the neighbouring regions. Furthermore, the non-uniformity in the optical thickness of such a layer prevents its intended use as wave plate. In order to favour lateral rotation instead of tilting, a dielectric layer is inserted in between the electrodes and the liquid crystal layer. This layer shields the liquid crystal from the regions above the electrodes with strong vertical electric fields. Figure 8(b) shows that a more homogeneous distribution of the liquid crystal director is achieved when a dielectric layer is included. The dielectric layer is crucial for the operation of the device and is included for all results presented in this paper.

4.2. Switching times of the device

In figure 9 the evolution of the average twist is plotted versus time for a range of applied voltages. The average twist is the mean value of the director twist angle at all nodes of the irregular mesh. The initial director orientation is chosen parallel to the y -axis (a twist of $\pi/2$), and the succeeding driving configurations $C_1 - C_2 - C_3 - C_1 - C_2 - C_3 - C_1$ are applied, each for a duration of 250 ms. The first period with C_1 applied is not strictly necessary since the director is already aligned along the y -direction. It is added to illustrate that the average director in this configuration remains along the y -direction. The minimum voltage required to rotate the director over an angle of 2π is 4 V. Near the rotation threshold, the switching time is larger than 250 ms. The switching time decreases with increasing voltage.

The evolution of the average twist from one driving configuration to the next follows approximately an exponential decay. Table 1 gives the time constant of this exponential decay, which is a measure of the device speed. In the top row of the first column, the time constant is given for the device with an applied voltage of 5 V. The reported switching time is quite large. However, a reduction of the time constant can be achieved by several means, as illustrated in the table. Increasing the driving voltage, as shown in the bottom row of the table, is an obvious means to lower the time constant. The stronger electric field results in a faster response of the liquid crystal. The dielectric layer lowers the electric field strength in the liquid crystal layer. Therefore reducing the thickness of the dielectric layer brings the liquid crystal closer to the electrodes and increases the field strength inside the liquid crystal layer, as illustrated in the second column. In the third column, the thickness of the dielectric layer d is kept the same as in the default case, but its dielectric constant ε is increased. Due to the discontinuity of the normal electric field at the interface, increasing the dielectric constant of the dielectric layer implies increasing the normal component of the electric field at the interface with the liquid crystal, leading to a faster response of the liquid crystal as illustrated in the table.

With the original device configuration the tilt angle of the director stays below $\pi/6$. For higher voltages, a higher dielectric constant, or a thinner dielectric layer the tilt increases up to angles of $\pi/3$. This has a profound effect on the homogeneity of the liquid crystal layer and thus on the applicability of the device as a reconfigurable wave plate. An alternative approach is to change the size and spacing of the hexagonal electrodes. In this case the time constant can be reduced without a significant increase in the average tilt angle as shown in the fourth column of table 1. The planar anchoring parameter W_η does not influence the switching time, but it limits the tilt angle near the surface.

Changing the liquid crystal layer thickness also affects the switching speed. The electric field is the strongest at the bottom of the liquid crystal. For a thicker liquid crystal layer the time constant is expected to increase due to the lower driving fields at the top. This agrees with the time constant behaviour of other liquid crystal devices driven by horizontal electric fields [13]. Table 2 details the influence of the liquid crystal layer thickness on the speed of the device. For operation as a wave plate, a certain optical phase retardation is required, and changing the thickness of the liquid crystal layer is then not an option.

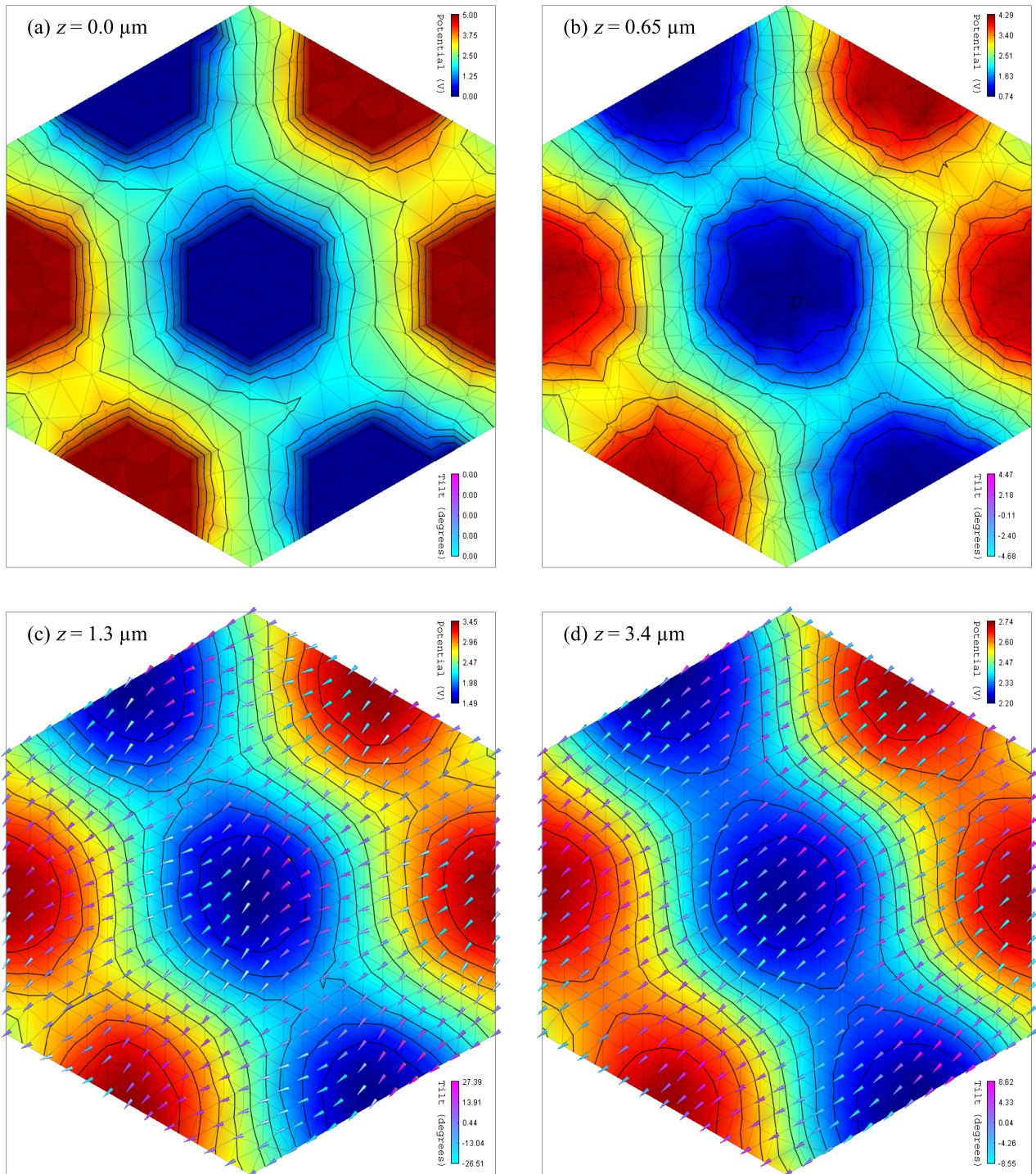


Figure 7. Director and potential distribution in different horizontal planes in the device at $t_1 = 500$ ms and driving configuration C_2 applied. Coordinate axes as defined in figures 1 and 2. Indication of the potential and director distribution are as in figure 6. (a) $z = 0.0 \mu\text{m}$: the xy -plane containing the electrodes at the bottom of the dielectric layer. (b) $z = 0.65 \mu\text{m}$: the plane in the middle of the dielectric layer. (c) $z = 1.3 \mu\text{m}$: the bottom plane of the liquid crystal layer. (d) $z = 3.4 \mu\text{m}$: the top plane of the liquid crystal layer.

Finally it is interesting to note that the liquid crystal parameters are not critical to device operation. In table 3 the switching time constant is compared for a number of different liquid crystal materials. The parameters of these liquid crystals differ over a broad range [12, 14, 15], but the device characteristics remain similar. The dominant influence on the time constant is the rotational viscosity γ_1 . For the liquid

crystals 6CHBT and 5CB, γ_1 is significantly lower, leading to smaller time constants.

4.3. Multistable wave plate

Figure 10 illustrates the multistable behaviour when the applied voltage of 5 V is removed after driving configurations C_1 , C_2

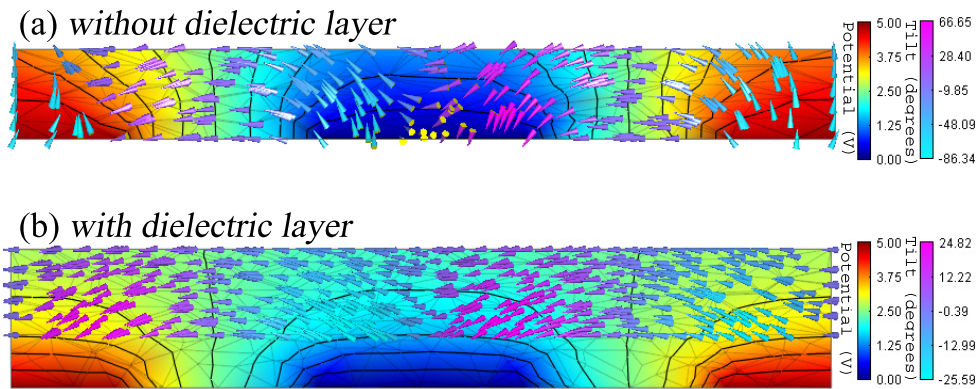


Figure 8. Distribution of the director in the xz -plane ($y = 0$ in figure 2) at $t_1 = 500$ ms when driving configuration C_2 is applied: (a) without the dielectric layer (the liquid crystal layer is positioned directly above the electrodes); (b) with a dielectric layer of $1.3 \mu\text{m}$ inserted between the electrodes and the liquid crystal layer.

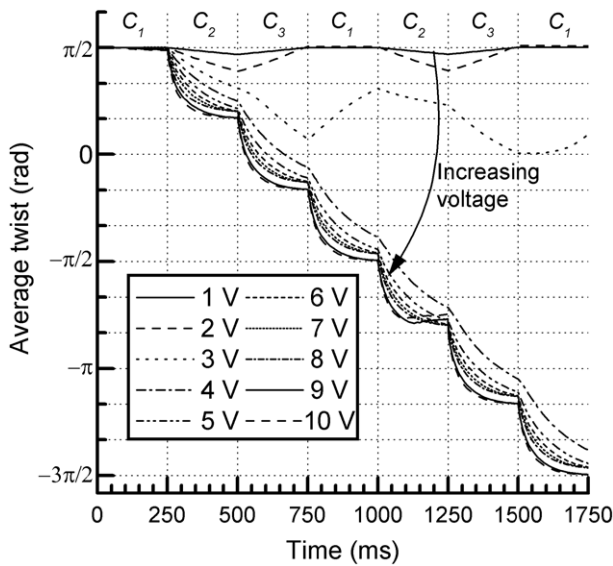


Figure 9. Variation of the average twist direction versus time for different voltages when applying the following sequence of driving configurations: $C_1 - C_2 - C_3 - C_1 - C_2 - C_3 - C_1$. Each driving configuration is applied for 250 ms, starting with the director aligned along the y -direction.

Table 1. Time constant of the exponential decay of the average twist with 5 and 10 V applied. Column 1 gives the time constant for the proposed device (default): thickness of the liquid crystal layer $2.1 \mu\text{m}$, thickness $d = 1.3 \mu\text{m}$ and dielectric constant $\epsilon = 3.5$ of the dielectric layer, dimensions and spacing of the hexagons $a = 3 \mu\text{m}$ and $b = 5 \mu\text{m}$. Column 2 shows the effect of reducing the thickness of the dielectric layer and column 3 of increasing its dielectric constant. Column 4 shows the effect of a change in the dimensions of the hexagonal electrodes and their spacing.

	Default	$d = 1.0 \mu\text{m}$	$\epsilon = 8.5$	$a = 5 \mu\text{m}$ $b = 3 \mu\text{m}$
5 V	117 ms	94 ms	49 ms	62 ms
10 V	36 ms	33 ms	24 ms	22 ms

or C_3 are applied. Time is measured relative to the instant where the driving voltage is removed. After 100 ms the director distribution relaxes to an orientation parallel to the surface along the average direction of the last driving configuration

Table 2. Time constant of the exponential decay of the average twist in the case of different thicknesses of the liquid crystal layer, for an applied voltage of 5 and 10 V. All other parameters are the same as in the default case shown in table 1.

	$1.0 \mu\text{m}$	$2.1 \mu\text{m}$	$3.0 \mu\text{m}$
5 V	80 ms	117 ms	166 ms
10 V	33 ms	36 ms	56 ms

Table 3. Time constant of the exponential decay of the average twist in the case of different liquid crystals for an applied voltage of 5 and 10 V. All other parameters are the same as in the default case shown in table 1.

	E7	ZLI-4792	5PCH	6CHBT	5CB
5 V	117 ms	115 ms	112 ms	88 ms	82 ms
10 V	36 ms	45 ms	37 ms	33 ms	30 ms

that was applied. The average direction of the director remains almost constant; however this direction is not exactly at an angle of $\pm\pi/6$ as expected. Figure 9 shows that a final direction closer to the desired angle is achieved by increasing the applied voltage or driving for a longer time. The evolution of the maximum and minimum twist gives an indication of the speed of the relaxation process and the homogeneity of the twist.

Relaxation is the most critical process in the device. After cooling down from the isotropic phase, a liquid crystal cell without rubbed alignment layers yields a Schlieren texture [1, 16] in which the director lies in the horizontal plane with a gradually varying orientation. Due to memory alignment, relaxation does not result in a homogeneous layer, but in the reconstruction of the original Schlieren texture. Memory alignment can be avoided using a slippery surface [5] at the top and bottom of the liquid crystal layer. This surface lowers the surface energy by preventing adsorption of the liquid crystal molecules to the surface. Developing materials to eliminate the memory alignment at the surface is a challenge for chemists. With a low anchoring strength along the y -axis ($W_\xi = 1 \times 10^{-6} \text{ J m}^{-2}$ and $\vec{\xi} = \vec{y}$), simulations have shown that in-plane rotation is still possible, but the threshold voltage and the time constant for rotation are increased.

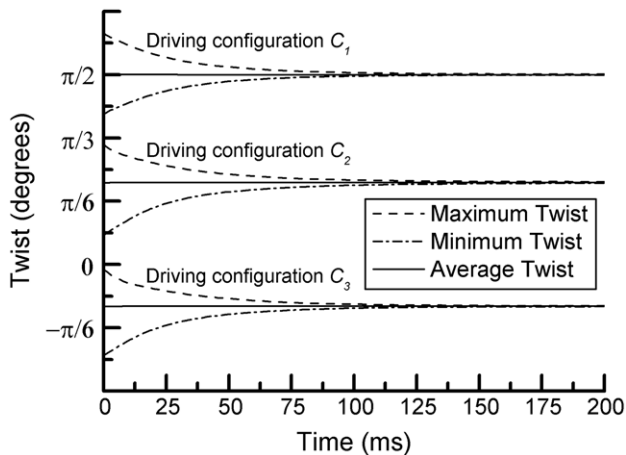


Figure 10. Maximum, minimum and average twist as a function of time after removing the applied voltages in the driving configurations C_1 , C_2 and C_3 .

5. Applications for the new liquid crystal device

The proposed device has a number of interesting capabilities, which are briefly discussed below.

5.1. Electrically driven multistable wave plate

The device acts as a rotating birefringent wave plate. Other device configurations that exhibit this characteristic have been proposed [3, 4], but the advantage of our device is the distribution of the electrodes over the whole surface of the device. In this way, the required driving voltages are lowered. Furthermore, there is no need for extra space next to the actual pixel to place the electrodes. The azimuthal degenerate anchoring surface enables the multistability of the device as explained above.

5.2. Hexagonal device with rubbed alignment layers

If the azimuthally degenerate planar anchoring surfaces at the top and bottom are replaced by anti-parallel rubbed alignment layers with the preferential director along the average horizontal electric field of one driving configuration, a director rotation over an angle of 2π is no longer possible and the multistability disappears. On the other hand, the azimuthal angle now becomes continuously adjustable between $-\pi/3$ and $\pi/3$ about the rubbing direction by applying one of the other two driving configurations. The amount of rotation can be controlled by the strength of the applied electric field.

When the electric field is turned off, the elastic force stemming from the alignment at the boundaries will align the director in the liquid crystal homogeneously. By applying the driving configuration with average horizontal field parallel to the anchoring direction for a short time, the director is forced back into the off-state and thus the switching off time is decreased.

5.3. Electric field driven alignment direction

Some new types of liquid crystal devices are based on switching between parallel and twisted states [17, 18]. Our new

device can handle this type of switching. Decreasing the dimensions of the electrodes and the spacing between them lowers the effect of the driving field at the top substrate. The electrodes create an electric field at the bottom of the liquid crystal layer which forms a switchable alignment direction. A strong anchoring alignment layer on the top substrate in combination with such a switchable alignment at the bottom of the liquid crystal makes it possible to switch between the parallel and twisted state.

6. Conclusions

A new type of liquid crystal device with the ability to rotate the liquid crystal director over 2π in the plane parallel to the glass substrates has been proposed and its feasibility demonstrated. Switching of the liquid crystal is induced by horizontal fields between electrodes in a honeycomb arrangement. This device can be used as a rotating wave plate in optical setups. The electric field distribution within the liquid crystal is similar to the distribution in the in-plane switching mode of liquid crystals, but the direction of switching is controllable. Removal of the electric field does not result in a return to the original configuration, but instead the layer relaxes to a uniform birefringent layer with the uniaxial axis oriented along the average azimuthal direction of the driving configuration before switching off.

Besides the application as a controllable wave plate, further applications such as an electric field driven alignment layer are feasible. Replacement of the surface anchoring with rubbed alignment layers makes the rotation continuously adjustable over a limited range. A continuous rotation to any specified angle might be possible, but requires further investigation of the rotation and relaxation processes.

Acknowledgments

The research of C Desimpel is funded by a PhD grant of the Institute for the Promotion of Innovation through Science and Technology in Flanders (IWT-Vlaanderen). The research is a result of collaboration within the framework of the European Research Training Network SAMPA and the Interuniversity Attraction Pole program PHOTON-network of the Belgian Science Policy. J Beeckman and H Desmet are funded by the Fund for Scientific Research (FWO-Vlaanderen).

References

- [1] De Gennes P G and Prost J 1995 *The Physics of Liquid Crystals* (Oxford: Oxford University Press) pp 102, 133, 134, 163
- [2] Lueder E 2001 *Liquid Crystal Displays: Addressing Schemes and Electro-Optical Effects* (Chichester: Wiley) p 116
- [3] Davidson A J, Elston S J and Raynes E P 2005 *J. Phys. D: Appl. Phys.* **38** 376
- [4] Kim J H, Yoneya M and Yokoyama H 2002 *Nature* **420** 159
- [5] Dozov I, Stoenescu D N, Lamarque-Forget S, Martinot-Lagarde Ph and Polossat E 2000 *Appl. Phys. Lett.* **77** 4124
- [6] Bryan-Brown G P, Wood E L and Sage I C 1999 *Nature* **399** 338
- [7] Ramdane O Ou, Auroy Ph, Forget S, Raspaud E, Martinot-Lagarde Ph and Dozov I 2000 *Phys. Rev. Lett.* **84** 3871

- [8] Zhao W, Wu C and Iwamoto M 2000 *Phys. Rev. E* **62** R1481
- [9] Fernández F A, Day S E, Trwoga P, Deng H F and James R 2002 *Mol. Cryst. Liq. Cryst.* **375** 297
- [10] Davies J B, Day S, DiPasquale F and Fernández F A 1996 *Electron. Lett.* **32** 582
- [11] Mori H, Gartland E C, Kelly J R and Bos P J 1999 *Japan. J. Appl. Phys.* **38** 135
- [12] Yeh P and Gu C 1999 *Optics of Liquid Crystal Displays* (New York: Wiley-Interscience) p 12
- [13] Oh-e M and Kondo K 1996 *Appl. Phys. Lett.* **69** 623
- [14] Sarkar P, Mandal P, Paul S, Paul R, Dabrowski R and Czuprynski K 2003 *Liq. Cryst.* **30** 507
- [15] Blinov LM and Chigrinov VG 1994 *Electrooptic Effects in Liquid Crystal Materials* (New York: Springer) p xiv
- [16] Dierking I 2003 *Textures of Liquid Crystals* (Weinheim: Wiley-VCH) p 51
- [17] Dozov I, Nobili M and Durand G 1997 *Appl. Phys. Lett.* **70** 1179
- [18] Xiang C Y Sun X W and Yin X J 2003 *Appl. Phys. Lett.* **83** 5154